Relaxing Symmetric Multiple Windows Stereo Using Markov Random Fields

Andrea Fusiello[1], Umberto Castellani[1], and Vittorio Murino[1]

Dipartimento di Informatica, Università di Verona
Strada le Grazie 15, 37134 Verona, Italy
{fusiello,castellani,murino}@sci.univr.it

Abstract. This paper introduces R-SMW, a new algorithm for stereo matching. The main aspect is the introduction of a Markov Random Field (MRF) model in the Symmetric Multiple Windows (SMW) stereo algorithm in order to obtain a non-deterministic relaxation. The SMW algorithm is an adaptive, multiple window scheme using left-right consistency to compute disparity. The MRF approach allows to combine in a single functional the disparity values coming from different windows, the left-right consistency constraint and regularization hypotheses. The optimal estimate of the disparity is obtained by minimizing an energy functional with simulated annealing. Results with both synthetic and real stereo pairs demonstrate the improvement over the original SMW algorithm, which was already proven to perform better than state-of-the-art algorithms.

1 Introduction

Three-dimensional (3D) reconstruction is a fundamental issue in Computer Vision, and in this context, structure from stereo algorithms play a major role. The process of stereo reconstruction aims at recovering the 3D scene structure from a pair of images by searching for *conjugate points*, i.e., points in the left and right images that are projections of the same scene point. The difference between the positions of conjugate points is called *disparity*.

Stereo is a well known issue in Computer Vision, to which many articles have been devoted (see [4] for a survey). In particular, the search for conjugate points in the two images is one of the main problem, and several techniques have been proposed to make this task more reliable. The search is based on a matching process that estimates the "similarity" of points in the two images on the basis of local or punctual information. Actually, feature-based methods try to associate image features (e.g., corners) in the image pair, whereas area-based methods try to find point correspondences by comparing local information. The main difference lies in the fact the the former approach produces a sparse (i.e., only in correspondence of features) disparity map, whereas, the latter generates a dense disparity image. In particular, the area-based matching process is typically based on a similarity measure computed between small windows in two images (left and

M.A.T. Figueiredo, J. Zerubia, A.K. Jain (Eds.): EMMCVPR 2001, LNCS 2134, pp. 91–105, 2001.

right). The match is normally found in a deterministic way, in correspondence of the highest similarity value.

In this paper, a novel probabilistic stereo method is proposed, which is based on the *Symmetric Multi-Window*(SMW) algorithm presented in [7,8]. In this algorithm, matching is performed by correlation between different kinds of windows in the two images, and by enforcing the so-called *left-right consistency* constraint. This imposes the uniqueness of the conjugate pair, i.e., each point on one image can match at most one point on the other image. This algorithm is fully deterministic and exhibits good performances, as compared with the state of the art, namely [15,23]. Still, there is margin for improvement (as our results show) by implementing a probabilistic SMW using Markov Random Fields (MRFs). To this end, SMW has been re-designed in a probabilistic framework by defining a random field evolving according to a suitable energy function.

Literature about MRFs is large and covers many topics of image processing, like restoration, segmentation, and image reconstruction considering both intensity (video) [3] and range images [1]. In addition, different approaches, closer in spirit to ours, were proposed aimed at integrating additional information in the MRF model, like, for instance, edges to guide the line extraction process [10], or confidence data to guide the the reconstruction of underwater acoustic images [19].

More specifically, MRFs are also frequently used in computer vision applications in the context of stereo or motion. For example, in [14] the motion vector is computed adopting a stochastic relaxation criterion, or, in [16], MRFs are used to detect occlusions in image sequences. Stereo disparity estimation methods using MRFs have been proposed in several papers. In [21], a stereo matching algorithm is presented as a regularized optimization problem. Only a simple correspondence between single pixels in the image pair is considered that leads to an acceptable photometric error, without exploiting local information for disparity estimation. In [17], matching is based on a fixed single correlation window, shifted along raster scan lines, and disparity is calculated by integrating gradient information in both left and right images. In this way, a mix between area- and feature-based matching is obtained, but occlusions are not managed by the algorithm. In [22], an MRF model was designed to take into account occlusions defining a specific dual field, so that they can be estimated in a similar way as in a classic *line process* similar to that presented in [12].

In our approach, for each pixel, different windows are (ideally) considered to estimate the Sum of Squared Differences (SSD) values and related disparities. When using area-based matching, the disparity is correct only if the area covered by the matching window has constant depth. The idea is that a window yielding a smaller SSD error is more likely to cover a constant depth region; in this way, the disparity profile itself drives the selection of an appropriate window.

The main contribution of this paper lies in the definition of a MRF model for a non-deterministic implementation of the SMW algorithm, in order to consider in a probabilistic way the contributions associated to the several windows, also introducing a local smoothness criterion. The initial disparity is computed for

each window with SSD matching, then the *Winner-Take-All* approach of the SMW algorithm is relaxed by exploiting the MRF optimization.

The rest of the paper is organized as follow. In Section 2, the stereo process is described, and the MRF basic concepts are reported in Section 3. The actual MRF model is detailed in Section 4, and results are presented in Section 5. Finally, in Section 6, conclusions are drawn.

2 The Stereo Process

Many algorithms for disparity computation assume that conjugate pairs lie along raster lines. In general this is not true, therefore stereo pairs need to be *rectified* – after appropriate camera calibration – to achieve epipolar lines parallel and horizontal in each image [9].

A customary assumption, moreover, is that the image intensity of a 3D point is the same on the two images. If this is not true, the images must be *normalized*. This can be done by a simple algorithm [2] which computes the parameters of the gray-level transformation

$$I_l(x, y) = \alpha I_r(x, y) + \beta \qquad \forall (x, y)$$

by fitting a straight line to the plot of the left cumulative histogram versus the right cumulative histogram.

The matching process consist in finding the element (a point, region, or generic feature) in the right image which is most similar, according to a similarity metric, to a given element in the left image.

In the simple correlation stereo matching, similarity scores are computed, for each pixel in the left image, by comparing a fixed window centered on the pixel, with a window in the right image, shifting along the raster line. It is customary to use the Euclidean distance, or Sum of Squared Differences (SSD), as a (dis)similarity measure. The computed disparity is the one that minimizes the SSD error.

Even under simplified conditions, it appears that the choice of the window size is critical. A too small window is noise-sensitive, whereas an exceedingly large one acts as a low-pass filter, and is likely to miss depth discontinuities. This problem is addressed effectively – although not efficiently – by the Adaptive Window algorithm [15], and by the simplified version of the multiple window approach, introduced by [13,11].

Several factors make the correspondence problem difficult. A major source of errors in computational stereo are occlusions, although they help the human visual system in detecting object boundaries. Occlusions create points that do not belong to any conjugate pairs (Figure 1). There are two key observations to address the occlusions issue: (i) matching is not a symmetric process. When searching for corresponding elements, only the visible points in the reference image (usually, the left image) are matched; (ii) in many real cases a disparity discontinuity in one image corresponds to an occlusion in the other image. Some

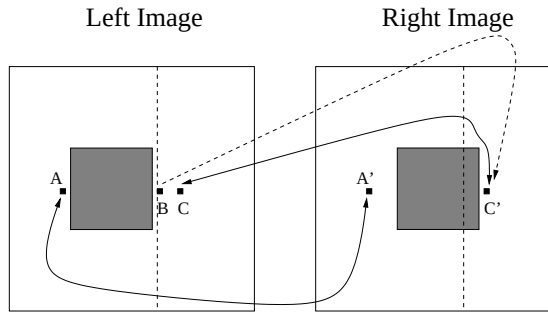

Fig. 1. Left-right consistency in the case of the random-dot stereogram of Figure 3. Point B is given C' as a match, but C' matches $C \neq B$.

authors [6,5] use the observation (i) to validate matching (left-right consistency); others [11,2] use (ii) to constrain the search space.

Recently, a new algorithm has been proposed [8] that computes disparity by exploiting both the multiple window approach and the left-right consistency constraint. For each pixel, SSD matching is performed with nine 7×7 windows with different centers: the disparity with the smallest SSD error value is retained.

The idea is that a window yielding a smaller SSD error is more likely to cover a constant depth region. Consider the case of a piecewise-constant surface: points within a window covering a surface discontinuity come from two different planes, therefore a single "average" disparity cannot be assigned to the whole window without making a manifest error. The multiple windows approach can be regarded as a robust technique able to fit a constant disparity model to data consisting of piecewise-constant surface, that is, capable of discriminate between two different populations. Occlusions are also detected, by checking the left-right consistency and suppressing unfeasible matches accordingly.

In this work we introduce a relaxation of the SMW algorithm using MRF. Both the multiple windows and the left-right consistency constraint features are kept but, in some sense, they are relaxed.

As for the multiple windows, one may note that correlation needs to be computed only once, because an off-centered window for a pixel is the on-centered window for another pixel. Therefore, the multiple windows technique used by the SMW reduces to assign a given pixel the disparity computed for one of its neighbors with an on-centered window, namely, the neighbour with the smallest SSD error. The nine 7×7 windows scheme gives forth to a sparse neighbourhood of nine pixels. The idea is to relax this scheme, and consider the pixel with the smallest SSD error in a full $n \times n$ neighbourhood (Figure 2).

As for the left-right consistency, we noticed that in presence of large amount of noise or figural distortion, the left-right consistency could fail for true conjugate pairs, and points could be wrongly marked as occluded. In this respect, it would be useful to relax the constraint, allowing for small errors.

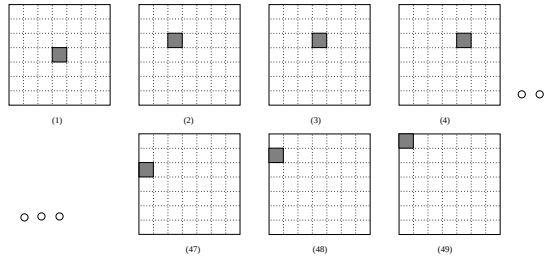

Fig. 2. The 49 asymmetric correlation windows for a 7×7 neighbourhood. The pixel for which disparity is computed is highlighted. The off-centered window for the highlighted pixel is the on-centered window for another pixel.

All these requests can be cast in terms of cost functions to be minimized over a disparity field, and this points strongly to Markov Random Fields.

3 Markov Random Fields

In this section will shall briefly review some basic concepts regarding MRF, in order to introduce our notation.

A MRF is defined on a finite lattice field I of elements i called sites (in our case, image pixels). Let us define a family of random variables $D=\{D_i= d_i,\ i\in I\}$, and let us suppose that each variable may assume values taken from a discrete and finite set (e.g., grey levels set). The image is interpreted as a realization of the discrete stochastic process in which pixel i is associated to a random variable D_i (being d_i its realization), and where, owing to the Markov property, the conditional probability $P\left(d_i \mid d_{I-\{i\}}\right)$ depends only on the value on the neighboring set of i, N_i (see [12]).

The Hammersley-Clifford theorem establishes the Markov-Gibbs equivalence between MRFs and Gibbs Random Fields [18], so the probability distribution takes the following form:

$$P\left(d\right) = Z^{-1} \cdot e^{-\beta \cdot U(d)} \tag{1}$$

where Z is a normalization factor called partition function, β is a parameter called temperature and *U(d)* is the energy function, which can be written as a sum of local energy potentials dependent only on the cliques $c\in C$ (local configurations) relative to the neighboring system [12]:

$$U\left(d\right) = \sum_{c \in C} V_c\left(d\right) \tag{2}$$

In general, given the observation g, the posterior probability *P(d | g)* can be derived from the Bayes rule by using the a-priori probability *P(d)* and the conditional probability *P(g | d)*. The problem is solved computing the estimate d according to a Maximum A-Posteriori (MAP) probability criterion. Since the

posterior probability is still of the Gibbs type, we have to minimize $U(d \mid g) = U(g \mid d) + U(d)$, where $U(g \mid d)$ is the *observation model* and $U(d)$ is the *a-priori model* [12]. Minimization of the functional $U(d \mid g)$ is performed by a simulated annealing algorithm with Metropolis sampler [20][18].

When the MRF model is applied to image processing the observation model describes the noise that degrades the image and the a-priori model describes the a-priori information independent from the observations, like, for instance, the smoothness of the surfaces composing the scene objects.

4 Model Description

To deal with the stereo problem the scene is modeled as composed by a set of planes located at different distances to the observer, so that each disparity value corresponds to a plane in scene. Therefore, the a-priori model is piecewise constant [18]. The observation model is harder to define because the disparity map is not produced by a process for which a noise model can be devised.

Whilst the a-priori model imposes a smoothness constraint on the solution, the observation model should describe how the observations are used to produce the solution. In fact, it is the observation term that encodes the **multiple windows** heuristic. For each site, we take into account all the disparity values in the neighbourhood, favouring the ones with the smallest SSD.

First a disparity map is computed using the simple SSD matching algorithm outlined in Sec. 2, taking in turn the left and the right images as the reference one. This produces two disparity maps, which we will call left and right, respectively. The **left-right consistency** constraint is implemented by coupling the left disparity and the right disparity values.

In order to define the MRF model, we introduce two random fields D^l and D^r to estimate the left and the right disparity map, two random fields G^l and G^r to model the left and the right observed disparity map, and two random field S^l and S^r to model the SSD error. The field D^l (or equivalently D^r) will yield the output disparity.

In the following we shall describe the MRF functional, by defining the the a-priori model, the observation model, and the left-right consistency constraint term. In the next two subsections, will shall omit superscript l and r in the field variables. It is understood that the a-priori model and the observation model applies to both left and right fields.

4.1 A-priori Model

With the a-priori term we encode the hypothesis that the surfaces in the scene are locally flat. Indeed, we employ a piecewise constant model, defined as:

$$U(d) = \sum_{i \in I} \sum_{j \in N_i} [1 - \delta(d_i, d_j)] \tag{3}$$

where d_i and d_j are the estimate disparities value (the realization of the field D) and the function $\delta(x, y)$ is defined as:

$$\delta(x, y) = \begin{cases} 1 & if \quad x = y \\ 0 & otherwise \end{cases} \tag{4}$$

This term introduces a regularization constraint, imposing that all pixels assume the same value in a region, thereby smoothing out isolated spikes.

4.2 Observation Model

In order to mimic the behaviour of the SMW algorithm, the observation model term introduces a local non-isotropic relaxation, favouring the neighbour observations with the lower SSD value:[1]

$$U(g, s \mid d) = \sum_{i \in I} \sum_{j \in N_i \cup \{i\}} [1 - \delta(d_i, g_j)] \cdot \left(\frac{1}{s_j}\right) \tag{5}$$

where g is the observation disparity map (the realization of the field G), s is the observed SSD values (the realization of the field S), and d is the disparity estimate (the realization of the field D). Following [18] the term $1 - \delta(x, y)$ represent a generalization of the sensor model for binary surface (derived by the binary symmetric channel theory).

In this term, the estimate value at site i, d_i, is compared with all its observed neighbours $\{g_j\}_{j \in N_i}$ and with g_i. When d_i takes the disparity of one (or more) of its neighbours, one (or more) term(s) in the sum vanishes. The lower is the SSD error of the chosen disparity, the higher is the cost reduction.

Please note that we are not relating the SSD value to the matching likelihood: the rationale behind this energy term is the multiple windows idea.

4.3 Left-Right Consistency Constraint Term

In our MRF model, besides an observation term and an a-priori term for both left and right disparity fields, we define a coupling term that settles the left-right constraint.

Let d_i^l be the left disparity (i.e., the disparity computed taking the left image as the reference) at site i, and d_i^r the right disparity at site i. The left-right consistency constraint states that:

$$d_i^l = -d_{i+d_i^l}^r. \tag{6}$$

The corresponding energy term is:

$$V(d^l, d^r) = \sum_{i \in I} \theta\left(d_i^l + d_{i+d_i^l}^r\right) \tag{7}$$

[1] Please note that SSD is an *error* measure, not a correlation or similarity measure.

where $\theta(x)$ is define as:

$$\theta(x) = \begin{cases} 0 & if \quad x = 0 \\ 1 & otherwise \end{cases} \tag{8}$$

In this way we introduces a payload when the left-right constraint is violated.

4.4 Final Model

The final MRF writes:

$$\begin{aligned} U\left(d^l, d^r \mid g^l, s^l, g^r, s^r\right) = & k_1 \cdot \left[U\left(g^l, s^l \mid d^l\right) + U\left(g^r, s^r \mid d^r\right)\right] + \\ & + k_2 \cdot \left[U\left(d^l\right) + U\left(d^r\right)\right] + \\ & + k_3 \cdot V\left(d^l, d^r\right) \end{aligned} \tag{9}$$

where $U\left(g^l, s^l \mid d^l\right)$ and $U\left(g^r, s^r \mid d^r\right)$ are the observation model applied to the left and right disparity reconstruction, $U\left(d^l\right), U\left(d^r\right)$ are the a-priori models and $V\left(d^l, d^r\right)$ is the left-right constraint term. Please note that these terms are all weighted by the coefficients k_1, k_2, k_3 heuristically chosen.

This model performs both simultaneously the left and right disparity reconstruction and the two estimates influence each other in a *cooperative* way. We call our algorithm Relaxed SMW (R-SMW).

5 Results

This section reports the main results of the experimental evaluation of our algorithm. Numerical and visual comparison with other algorithms are shown.

We first performed experiments on noise-free random-dot stereograms (RDS), shown in Figure 3. In the disparity maps, the gray level encodes the disparity,

(a) (b) (c) (d)

Fig. 3. Random-dot stereograms (RDS). The right image of stereogram (not shown here) is computed by warping the left one (a), which is a random texture, according to given disparity pattern: the square has disparity 10 pixel, the background 3 pixel. Disparity map computed with SSD matching (b), SSD values (c) and R-SMW disparity map.

(a) (b)

Fig. 4. "Head" stereo pairs from the Multiview Image Database, University of Tsukuba.

(a) (b)

Fig. 5. R-SMW disparity map (a) and ground truth (b).

that is the depth (the brighter the closer). Images have been equalized to improve readability.

Figure 3.b shows a disparity map computed by SSD matching with 7×7 fixed window. The negative effect of disparity jumps (near the borders of the square patch) is clearly visible. Accordingly, Figure 3.c shows that along the borders the SSD error is higher. R-SMW yields the correct disparity map, shown in Figure 3.d. This replicates exactly the result obtained by SMW [7]. We expect to appreciate the improvement brought by the MRF when noise affects the images, like in the real cases.

As a real example, we used the "Head" stereo pair shown in Figure 4, for which the disparity ground truth is given. The output of R-SMW is reported in Figure 5. The error image (Figure 6.a) shows in black the pixels where the disparity is different from the ground truth. For the others, the disparity value is shown as a gray level (the brighter the closer).

The R-SMW algorithms outputs two optimal disparity maps, the left and the right. By checking the left-right consistency against these two maps, one can

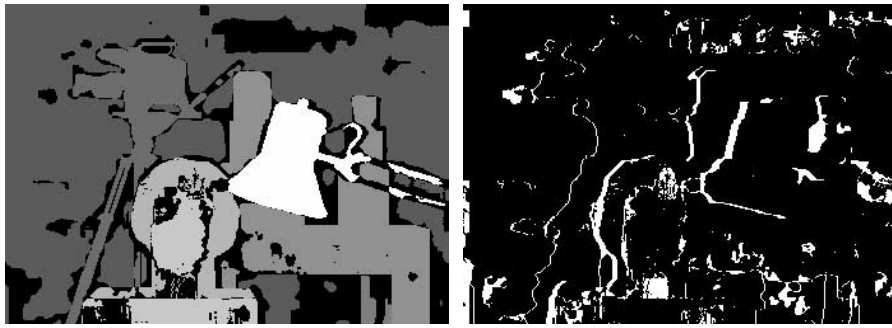

(a) (b)

Fig. 6. Error map (a): the wrong pixels are black, the other take the right disparity value. Occlusions map (b).

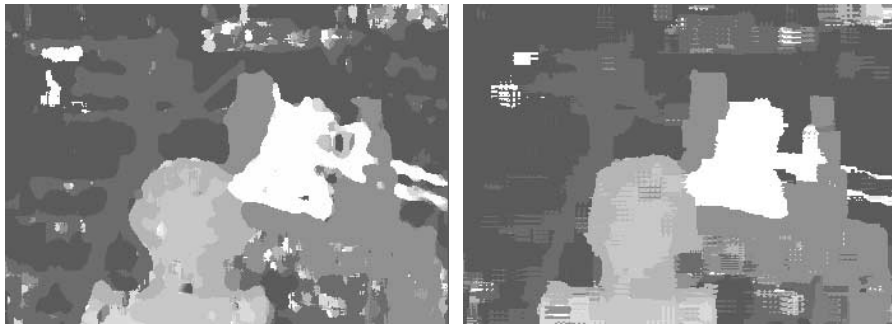

(a) (b)

Fig. 7. Disparity map calculated by Zabih and Woodfill algorithm (a) and through SMW algorithm (b).

detect occluded points. Figure 6 shows the occlusions map. It is worth noting that most of the wrong pixels of Figure 6.a comes from occlusions.

We compared R-SMW with SMW and our implementation of the Zabih and Woodfill algorithm (Figure 7). In the R-SMW result, the regions are more homogeneous and the edge are better defined. Moreover a lot of spurious points are cleared. Please note that there is a large wrong area, corresponding to a box on the shelf (top right). The ground truth disparity for that box is the same as the background, but all the stereo algorithms we tested agree in detecting a different disparity for the box. We suspect that the ground truth could be incorrect for that area.

For quantitative comparison, two error measures have been used: the Mean Absolute Error (MAE), i.e, the mean of absolute differences between estimated and ground true disparities, and the Percentage Error (PE), i.e., the percentage of pixel labeled with a wrong disparity. Table 1 reports the MAE and PE errors obtained on the "Head" stereo pair by SSD matching, Zabih and Woodfill algo-

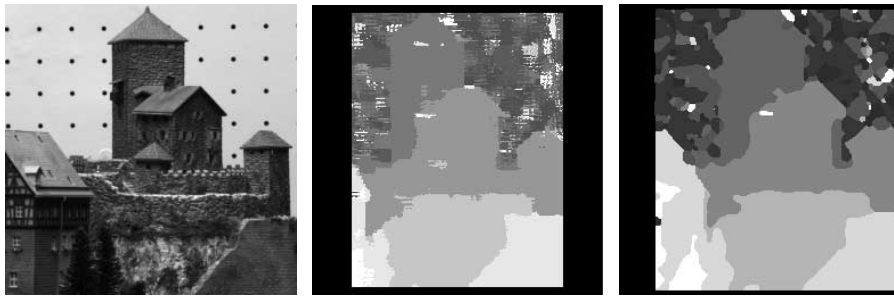

(a) (b) (c)

Fig. 8. "Castle" left image (a), SMW disparity (b), and R-SMW disparity (c).

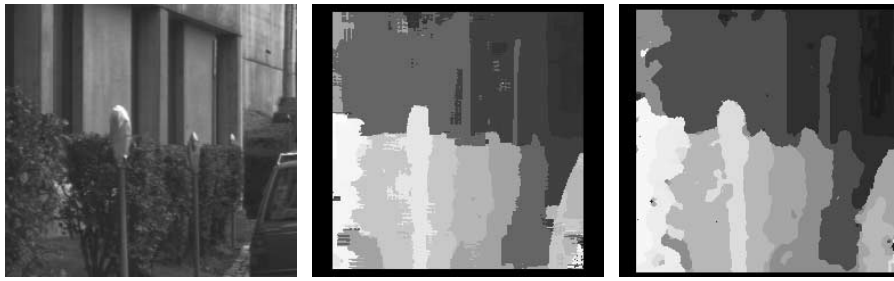

(a) (b) (c)

Fig. 9. "Parking meter" left image (a), SMW disparity (b), and R-SMW disparity (c).

rithm, SMW, and by R-SMW. Results are ordered by decreasing errors: R-SMW exhibit the best performance, improving over the SMW. The Zabih and Woodfill algorithm is very fast (it reaches 30 frames per second on dedicated hardware), but results suggest that accuracy is not its best feature. We did not compared R-SMW with the Adaptive Windows (AW) algorithm by Okutomi and Kanade [15], but in [7] SMW was already proven to be more accurate than AW.

Table 1. Error values obtained by the different disparity reconstruction algorithm.

Algorithm	MAE	PE
SSD with fixed window	0.8569	30.73%
Zabih and Woodfill	0.8012	31.56%
SMW	0.6194	24.98%
R-SMW	0.5498	21.33%

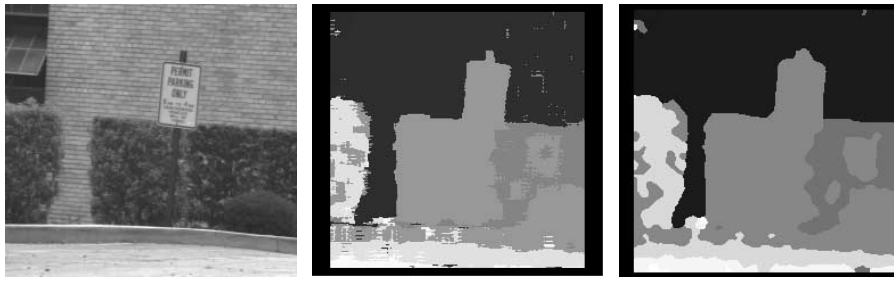

(a) (b) (c)

Fig. 10. "Shrub" left image (a), SMW disparity (b), and R-SMW disparity (c).

(a) (b) (c)

Fig. 11. "Trees" left image (a), SMW disparity (b), and R-SMW disparity (c).

We also report in Figures 8, 9, 10,and 12 the results of our algorithm on standard image pairs from the JISCT (JPL-INRIA-SRI-CMU-TELEOS) stereo test set, and from the CMU-CIL (Carnegie-Mellon University—Calibrated Imaging Laboratory). Although a quantitative evaluation was not possible on this image, the quality of our results seems to improve over SMW, especially because spurious points and artifacts are smoothed out.

6 Conclusions

We have introduced a relaxation of the SMW algorithm by designing a Markov Random Field where both the multiple windows scheme and the left-right consistency are embedded. Moreover, a regularization constraint is introduced, as customary, to bias the solution toward piecewise constant disparities. Thanks to the MRF versatility, all these constraints are easily expressed in terms of energy, and the final solution benefits from the trade off between a-priori model and observations. Indeed, results showed that R-SMW performs better than state-of-the-art algorithms, namely SMW, Zabih and Woodfill and (indirectly) AW.

(a) (b) (c)

Fig. 12. "Trees" left image (a), SMW disparity (b), and R-SMW disparity (c).

A sequential implementation of a MRF is computational intensive, of course: our algorithm took several minutes to converge to a solution, on the examples shown in the previous section. On the other hand, it reaches a high accuracy, and in some applications (eg. model acquisition), one might want to trade accuracy for time.

A drawback of R-SMW is that coefficients in the energy functional need to be adjusted heuristically, and their value is fairly critical for the overall quality of the result. Work is in progress to implement a procedure for selecting the best coefficients automatically.

Acknowledgements

The authors thank Daniele Zini who wrote the implementation in C of the Zabih and Woodfill algorithm. The "Castle" images were provided by the Calibrated Imaging Laboratory at Carnegie Mellon University (CMU-CIL), supported by ARPA, NSF, and NASA. The "Head" images with ground truth, from the Multiview Image Database, are courtesy of Dr. Y. Otha, University of Tsukuba. Thanks to the anonymous referees who made useful comments.

References

1. G.S Nadabar A.K. Jain. Range image segmentation using MRF models. In A.K. Jain and R. Chellappa, editors, *Markov Random Fields Theory and Application*, pages 542–572. Academic Press, 1993.
2. I. J. Cox, S. Hingorani, B. M. Maggs, and S. B. Rao. A maximum likelihood stereo algorithm. *Computer Vision and Image Understanding*, 63(3):542–567, May 1996.
3. H. Derin and H. Elliot. Modeling and segmentation of noisy and textured images using Gibbs random fields. *IEEE Trans. on Pattern Analysis and Machine Intelligence*, 9(1):39–54, 1987.
4. U. R. Dhond and J. K. Aggarwal. Structure from stereo – a review. *IEEE Transactions on Systems, Man and Cybernetics*, 19(6):1489–1510, November/December 1989.

5. O. Faugeras, B. Hotz, H. Mathieu, T. Viéville, Z. Zhang, P. Fua, E. Théron, L. Moll, G. Berry, J. Vuillemin, P. Bertin, and C. Proy. Real-time correlation-based stereo: algorithm, implementation and applications. Technical Report 2013, Unité de recherche INRIA Sophia-Antipolis, August 1993.
6. P. Fua. Combining stereo and monocular information to compute dense depth maps that preserve depth discontinuities. In *Proceedings of the International Joint Conference on Artificial Intelligence*, pages 1292–1298, Sydney, Australia, August 1991.
7. A. Fusiello, V. Roberto, and E. Trucco. Efficient stereo with multiple windowing. In *Proceedings of the IEEE Conference on Computer Vision and Pattern Recognition*, pages 858–863, Puerto Rico, June 1997. IEEE Computer Society Press.
8. A. Fusiello, V. Roberto, and E. Trucco. Symmetric stereo with multiple windowing. *International Journal of Pattern Recognition and Artificial Intelligence*, 14(8):1053–1066, December 2000.
9. A. Fusiello, E. Trucco, and A. Verri. A compact algorithm for rectification of stereo pairs. *Machine Vision and Applications*, 12(1):16–22, 2000.
10. E. Gamble and T. Poggio. Visual integration and detection of discontinuities: the key role of intensity edge. A.I. Memo 970, Massachusetts Institute of Technology, 1987.
11. D. Geiger, B. Ladendorf, and A. Yuille. Occlusions and binocular stereo. *International Journal of Computer Vision*, 14(3):211–226, April 1995.
12. S. Geman and D. Geman. Stochastic relaxation, Gibbs distribution, and Bayesian restoration of images. *IEEE Trans. on Pattern Analysis and Machine Intelligence*, 6(6):721–741, 1984.
13. S. S. Intille and A. F. Bobick. Disparity-space images and large occlusion stereo. In Jan-Olof Eklundh, editor, *European Conference on Computer Vision*, pages 179–186, Stockholm, Sweden, May 1994. Springer-Verlag.
14. J.Konrad and E.Dubois. Bayesian estimation of motion vector field. *IEEE Transactions on Pattern Analysis and Machine Intelligence*, 14(9):910–927, September 1992.
15. T. Kanade and M. Okutomi. A stereo matching algorithm with an adaptive window: Theory and experiments. *IEEE Transactions on Pattern Analysis and Machine Intelligence*, 16(9):920–932, September 1994.
16. A.Das K.P.Lim, M.N.Chong. A new MRF model for robust estimate of occlusion and motion vector fields. In *International Conference on Image Processing*, 1997.
17. K.G. Lim and R. Prager. Using Markov random field to integrate stereo modules. Technical report, Cambridge University Endineering Department, 1992. Available from http://svr-www.eng.cam.ac.uk/reports.
18. J. K. Marroquine. *Probabilistic Solution of Inverse Problem.* PhD thesis, Massachusetts Institute of Technology, 1985.
19. V. Murino, A. Trucco, and C.S. Regazzoni. A probabilistic approach to the coupled reconstruction and restoration of underwater acoustic images. *IEEE Transactions on Pattern Analysis and Machine Intelligence*, 20(1):9–22, January 1998.
20. C.D. Gellat Jr S. Kirkpatrik and M.P. Vecchi. Optimization by simulated annealing. *Science*, 220(4):671–680, 1983.
21. S.T.Barnard. Stereo matching. In A.K. Jain and R. Chellappa, editors, *Markov Random Fields Theory and Application*, pages 245–271. Academic Press, 1993.
22. W. Woo and A. Ortega. Stereo image compression with disparity compensation using the MRF model. In *Proceedings of Visual Communications and Image Processing (VCIP'96)*, 1996.

23. R. Zabih and J. Woodfill. Non-parametric local transform for computing visual correspondence. In *Proceedings of the European Conference on Computer Vision*, pages 151–158, Stockholm, 1994.